Agglomeration of mesoscopic particles in plasma

New Journal of Physics
The open-access journal for physics

Agglomeration of mesoscopic particles in plasma

B M Annaratone[1,3], Y Elskens[1], C Arnas[1], T Antonova[2], H M Thomas[2] and G E Morfill[2]

[1] PIIM, Université de Provence, Campus St. Jérôme, case 321, F-13397 Marseille, France
[2] Max-Planck Institut für Extraterrestrische Physik, D-85741 Garching, Germany
E-mail: bma@mpe.mpg.de

New Journal of Physics **11** (2009) 103013 (10pp)
Received 30 July 2009
Published 5 October 2009
Online at http://www.njp.org/
doi:10.1088/1367-2630/11/10/103013

Abstract. We disclose the basic mechanism of agglomeration of nano-sized particles. While for weakly coupled, mono-dispersed particles the electrostatic agglomeration has always been found to be unlikely, in strongly coupled complex (dusty) plasmas the occupation of positive states for small particles is relevant, leading to electrostatic attraction between differently charged particles. The occupation of positively charged states is further enhanced by dispersed distribution of size. The smaller particles are trapped by the larger, the accretion of which gives a positive feedback on the probability of positively charged small grains and then further accretion. Experiments on growth of carbon particles from sputtered graphite in RF and dc Argon plasma confirm the general theoretical prediction when the energy of the ions corresponds to plasma boundaries.

Contents

[3] Author to whom any correspondence should be addressed.

This paper addresses the agglomeration of mesoscopic size particles in ionized media, an important step in the process of formation of solid matter from free atoms and ions. The issue is of fundamental physics interest as well as relevant for the astrophysics community because the formation of dust occurs before the formation of stellar objects and planets. It may be important in diverse environments such as dust molecular clouds, proto-planetary nebulae, stellar outburst, comets, etc [1, 2]. In plasma processing of materials, the formation and growth of dust prevent the development of new technologies [3] although for certain applications it is advantageously exploited [4]. The agglomeration of dust may be important in fusion devices; nano-particles could escape through filters and convey tritium or activated material into the environment [5]. There is relevance to the formation of soot in exhaust gas and pollution: in general, larger particles are less dangerous for health and reduce chemical reaction risk. On another point of view, mesoscopic particles are now used for the under-skin assimilation of pharmaceuticals.

The growth of material from dispersed atoms consists in a preliminary phase of nucleation followed by deposition (of atomic material to the surface of already nucleated particles) and several processes of agglomeration, among which there is a first agglomeration process for small particles in the nano-size range, the object of this paper, and another for particles of dimensions comparable to the Debye length, to be considered in a forthcoming publication. For still larger particles, the agglomeration is almost uniquely related to high kinetic energies or strong confinement. While the nucleation process belongs to atomic physics, in which quantum effects are involved, the nano-scale agglomeration belongs to mesoscopic physics, the size scale where quantum and classical worlds coexist. Here, the solid surface can be approximated by the continuum (10^4–10^5 atoms in a 5 nm grain) but the discretization of the charge cannot be ignored. On average, classical models of ion collection by dust particles still hold; however, the attraction of particles is dominated by the instantaneous value of the charge, which is subject to fluctuations.

The previous work on fluctuations includes [6]–[8] and references therein: the electrostatic agglomeration has always been found insufficient to explain the agglomeration observed in nature and in laboratory experiments; in most cases, fluctuations of charge have been coupled with turbulence and plasma oscillations. Kortshagen and Bhandarkar [9] analyses several effects that contribute to the positive charging, as UV photo-detachment, field emission, impact by excited atoms and secondary electron emission caused by electron impact. These effects were reported as essential for agglomeration although they are small in the agglomeration experiments reported in the following (they should be considered in other applications). In this paper, we prove that high agglomeration rates may derive directly from electrostatic attraction (here calculated self-consistently together with the condition of quasi-neutrality of the overall space) in distributions that are at the same time strongly coupled and dispersed in size. For distances among particles of the order of few nanometres, the attractive forces due to fluctuating electromagnetic fields corresponding to charge fluctuations inside the solid, van der Waals–Casimir forces [10], are comparable with classical electrostatic forces due to fluctuation of the electron and ion fluxes to the surface, see also [11, 12]. This study is beyond the aims of this paper, we only point out that in this respect the agglomeration rate presented in the present paper may be underestimated.

1. Charge for isolated particles

We consider dust particles embedded in plasma consisting of electrons and positive ions. In this model, a dust particle can be in states characterized by $Q(N) = Ne$, with N denoting the number of positive electron charges $+e$. Transitions to the state 'N' are associated with the probability to capture a positive ion, w_N^{i}, or an electron, w_N^{e}. They are calculated using the Boltzmann distribution for the repelled species and an orbital motion-limited (OML) cross section for the attracted species [13]. The OML theory does not involve space charge, so it is applicable for low level of fluxes. It is applicable for small enough isolated grain, with radius $r_{\mathrm{p}} \ll \lambda_{\mathrm{D}}$, where λ_{D} is the electron Debye length [14]. The typical distance for the use of this theory in presence of other objects, as in complex plasmas, is given in [15]; replacing the floating potential with the vacuum approximation $V(N) = eN/(4\pi\varepsilon_0 r_{\mathrm{p}})$, the validity of this model is limited by $r_{\mathrm{p}}[-e^2N/(4\pi\varepsilon_0 r_{\mathrm{p}} k_{\mathrm{B}} T_{\mathrm{i}})]^{1/2} < n_{\mathrm{d}}^{-1/3}$ (or $< \lambda_{\text{mean free path}}$), with T_{i} the temperature of the ions and n_{d} the density of dust. Thus

$$w_N^{\alpha} = 4\pi r_{\mathrm{p}}^2 n_{\alpha} \sqrt{\frac{k_{\mathrm{B}} T_{\alpha}}{2\pi m_{\alpha}}}\, g\left(-\sigma_{\alpha} \frac{e^2 N}{4\pi\varepsilon_0 r_{\mathrm{p}} k_{\mathrm{B}} T_{\alpha}}\right), \tag{1}$$

where $m_{\mathrm{i}}(m_{\mathrm{e}})$ is the mass of ions (electrons), $\sigma_{\mathrm{i}} = +1$, $\sigma_{\mathrm{e}} = -1$ and $g(u) = 1 + u$ when $u \geqslant 0$ and $g(u) = e^u$ when $u \leqslant 0$. We extend the number of levels, from the most positive, N_{p}, to the most negative, N_{n}, until we find that w_N^{i} and w_N^{e} are negligible and formally set equal to zero. The system then forms a finite Markov chain of birth and death type, see e.g. [16], so that knowing the transition rates the solution for the equilibrium, i.e. stationary, probability of occupancy, $P_{\mathrm{eq}}(N)$, is explicit:

$$P_{\mathrm{eq}}(N) = P_{\mathrm{eq}}(N_{\mathrm{p}}) \prod_{N'=N+1}^{N_{\mathrm{p}}} \left(\frac{w_{N'}^{\mathrm{e}}}{w_{N'-1}^{\mathrm{i}}}\right) \tag{2}$$

with $P_{\mathrm{eq}}(N_{\mathrm{p}})$ determined by the normalization: $\sum_{N=N_{\mathrm{n}}}^{N_{\mathrm{p}}} P_{\mathrm{eq}}(N) = 1$. A typical distribution of occupancy of the states for different particle sizes can be found in figure 1, where the most probable states scale duly as r_{p}. We show also the strong dependence of the charge on the ion temperature. The average time of permanence in the states, $\tau_N = 1/(w_N^{\mathrm{i}} + w_N^{\mathrm{e}})$, has been also plotted and there is enough time, typically $> 10^{-4}$ s, for electrostatic attraction when one small particle is positive, $N \geqslant 1$. However, as predicted in the literature, states near the upper and lower ends of the distribution are rarely occupied so that the probability of occupancy of positive states is too low to allow agglomeration of particles in quasi-neutral plasma.

2. Charge in complex plasma

The condition $n_{\mathrm{i}} \gg n_{\mathrm{e}}$ is typical of plasma sheaths, but in this environment the strong electric fields prevent equilibrium stability for nano-sized particles. Instead in quasi-neutral complex plasmas, with increasing density of dust the most external part of the particles' sheaths begin to interact, $n_{\mathrm{e}}^{-1/3} \sim \lambda_{\mathrm{De}}$. Then the overall quasi-neutrality condition $n_{\mathrm{i}} = n_{\mathrm{e}} + \bar{Q} n_{\mathrm{d}}$, with $\bar{Q}$ the average dust charge, leads to electron depletion in the inter-particle space. We take this effect into account assuming that the electrons and ions attempting to reach the particles are in the same ratio as the averaged density ratio; in spherical geometry the space charge very near to the particles does not affect much the volume average. For interacting particles the

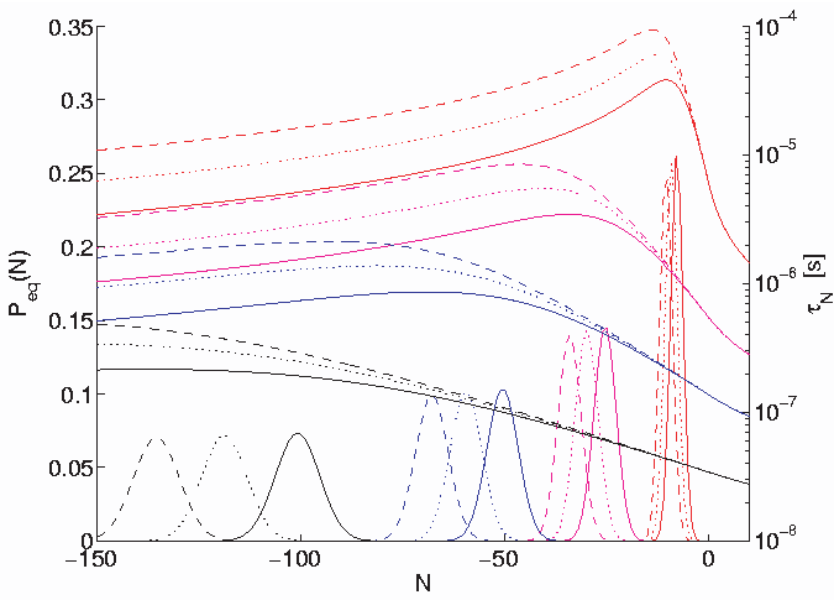

Figure 1. Peaked lines (left ordinates): occupation probability of the states (labelled by elementary charges) for isolated particles with radius $r_p = 1.5$, 5, 10 and 20 nm (from right to left), in plasma with $n_i = 2 \times 10^{16}\,\mathrm{m}^{-3}$, $T_e = 3\,\mathrm{eV}$, with $T_i = 0.3\,\mathrm{eV}$ (dashed lines), 0.1 eV (dotted lines) and 0.03 eV (solid lines). Flatter lines (right ordinates): permanence time, with curves from top downwards for same radii. Lines are guides to the eye.

equilibrium occupation of the states, equation (2), is recalculated with the electron densities in equation (1) different from the ion densities by a factor $K = n_i/n_e$. The average charge is then $\bar{Q}(K) = \sum_{N=N_n}^{N_p} P_{eq}(N, K)eN$, and the value for K is obtained solving the quasi-neutrality equation $K = 1 - \bar{Q}(K)n_d/(en_e)$ consistently with the occupation distribution of the states for a dust particle, for given: density of plasma (n_i), radius and density of dust and temperature of electrons and ions. In mono-dispersed assemblies the probability of positive dust increases with smaller particle size, larger n_i/n_d, larger T_i and smaller T_e. To describe the process of agglomeration the OML cross section [13] yields the rate:

$$A = n_d^2 r_p^2 \sqrt{\frac{k_B T_d}{2\pi M_d}} \sum_{N'=N_n}^{N_p} \sum_{N''=N_n}^{N_p} [1 - h(N'N'')] P_{eq}(N') P_{eq}(N'') \left(1 - \frac{e^2 N' N''}{4\pi \varepsilon_0 r_p k_B T_d}\right) \tag{3}$$

with M_d the mass of the particles and $h(x) = 1$ when $x > 0$ and 0 otherwise. This equation gives agglomeration rates always too low compared to the experimental formation time of particulate. To give typical experimental values, for $r_p = 5$ nm, $n_i = 10^{16}\,\mathrm{m}^{-3}$, $n_d = 2 \times 10^{15}\,\mathrm{m}^{-3}$, $T_e = 3\,\mathrm{eV}$ and $T_i = 0.1\,\mathrm{eV}$, we find $\bar{Q} = -4.83\mathrm{e}$ and $A = 8.66 \times 10^{-8}\,\mathrm{m}^{-3}\,\mathrm{s}^{-1}$; in the timescale of experiments (10^2 s), we would only reach a density of aggregates about $10^{10}\,\mathrm{m}^{-3}$.

3. Charge in dispersed distribution of sizes

When dust particles of different diameters coexist, the average density ratio of the ions over the free electrons, K, is strongly dominated by the larger particles. Here, we consider a bi-dispersed

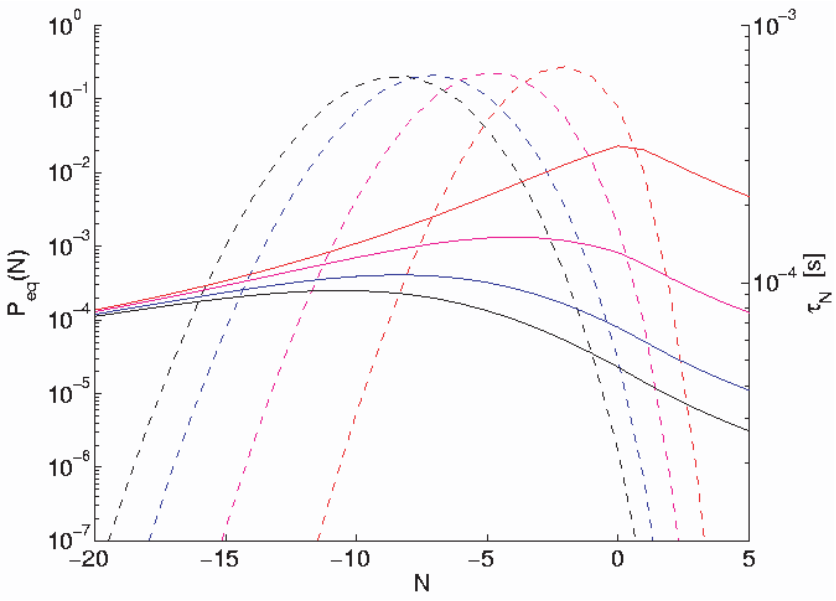

Figure 2. Occupation probability (dashed lines, left ordinates) of states for small ($r_s = 3$ nm) particles in presence of larger particles: from left to right $r_L = 3$, 10, 30 and 100 nm. Permanence time (solid lines, right ordinates) from top downwards. Here $n_i = 10^{16}\,m^{-3}$, $n_{ds} = 10^{15}\,m^{-3}$, $n_{dL} = 10^{14}\,m^{-3}$, $T_e = 3$ eV, $T_i = 0.3$ eV, $T_d = 0.03$ eV.

distribution of size, i.e. particles of two sizes (small, subscript s, and large, subscript L), so the neutrality condition is

$$K - 1 + \bar{Q}_s(K)\frac{n_{ds}}{n_e} + \bar{Q}_L(K)\frac{n_{dL}}{n_e} = 0. \tag{4}$$

Figure 2 shows the curves of the self-consistent occupation distribution for several larger particle sizes under typical conditions. It is clear that the probability to have a positive small particle increases with the size of the large particles. The agglomeration rate to a large particle is given by

$$A = n_{ds}^2 r_L^2 \sqrt{\frac{k_B T_d}{2\pi M_{ds}}} \sum_{N'=N_n}^{N_p} \sum_{N''=N_n}^{N_p} [1 - h(N'N'')] P_{eq,s}(N') P_{eq,L}(N'') \left(1 - \frac{e^2 N' N''}{4\pi\varepsilon_0 r_L k_B T_d}\right). \tag{5}$$

Several factors contribute to the agglomeration of particles of different sizes, as the probability of occupation of high negative charge states for the large particles, so that the electrostatic attraction is enhanced. High random fluxes for the small particles, high T_d and small masses, also play a favourable role.

4. Comparison with experiments

The theoretical model proposed explains the main features highlighted by the experiments. In short, at the beginning of the discharge, particles nucleate and grow by radical attachment; some agglomeration is still likely for very small particles. At 3–5 nm size, the electrostatic

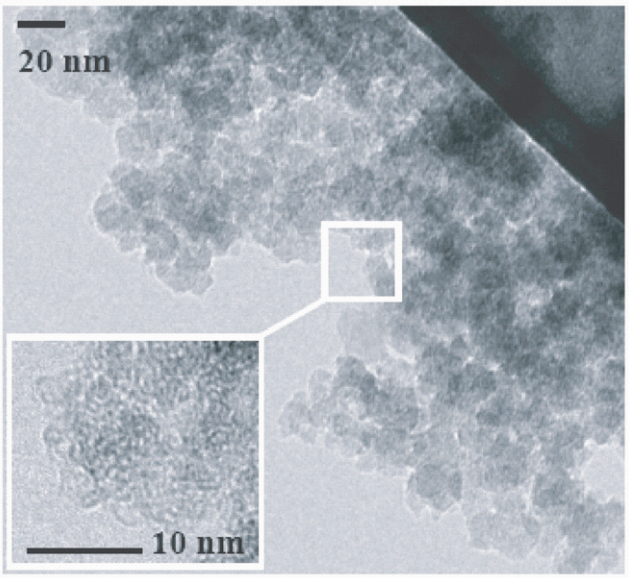

Figure 3. High-resolution transmission electron microscopy of a carbon particle collected after 30 s in dc argon discharge at 42 W and 60 Pa.

agglomeration is hindered by the negligible probability of occupation of the positive states, as a consequence the density of these particles increases. At particle densities comparable with the plasma density, some of the 3–5 nm particles become statistically positive making agglomeration again possible, and, with the growth, more and more effective. The fast growth stage is followed by a slower one when the trapping of small particles is limited by their production process. Thus the cross over in the growth rate has been identified as the transition between excess and shortage of small particles.

In the hypothesis of a binary distribution of size, we are able to reproduce the growth rate, Γ, starting from the plasma parameters; it is derived from the agglomeration rate as

$$\Gamma = A r_s^3/(2r_L^2). \tag{6}$$

During the process the balance equation for the small particles density is

$$F = \theta_d[n_{dL}A + (dn_{ds}/dt)], \tag{7}$$

where F is the flux of small particles continuously injected in the dust cloud, the thickness of which is θ_d. Therefore, the agglomeration rate at the beginning of the small particle depletion is $A_D = F/(n_{dL}\theta_d)$. Note that the validity of our assumptions can be checked by looking at the experimental data (they also must show internal consistency); the growth rate before the cross over, Γ, is linked to r_{LD} and F by

$$\Gamma = F r_s^3/(2r_{LD}^2 n_{dL}\theta_d). \tag{8}$$

As we now show, the results of the calculation agree quantitatively with the observations.

Let us analyse the experiments reported in [17, 18] and on-going at present. Dust particles grow in dc argon discharge at 42 W and 60 Pa from carbon atoms sputtered from the cathode. In this case, it is possible to identify agglomerates of several 3–5 nm particles, see figure 3. The growth of the agglomerate in this discharge has a rate cross over at about 45 nm; below

Table 1. Particle charges, agglomeration rates and growth rates of larger particles in presence of smaller ones. In each cell: top-left: $\bar{Q}_s$ (e); top-right: $\bar{Q}_L$ (e); bottom-left: A (s^{-1}); bottom-right: Γ(nm s^{-1}). Here, $r_{ds} = 1.5$ nm, $n_i = 10^{17}$ m^{-3}, $n_{dL} = 2 \times 10^{14}$ m^{-3}, $T_e = 2$ eV, $T_i = 0.1$ eV, $T_d = 0.035$ eV. Values in bold correspond to dc plasma experiment.

	r_L (nm)					
n_{ds}(m^{-3})	1.5	5	30	45	65	100
8.5×10^{16}	−1.15; −1.15	−1.14; −3.68	−1.10; −21.0	−1.08; −30.9	−1.05; −43.4	1.01; −64
	1.02; **0.76**	6.13; **0.41**	226; **0.42**	527; **0.43**	1150; 0.45	2924; 0.49
3.8×10^{16}	−2.47; −2.47	−2.44; −7.79	−2.28; −42.9	−2.19; −61.7	−2.08; −84.6	−1.91; −120
	0.038; 0.028	0.22; 0.015	11.3; 0.021	30.7; 0.026	80.5; **0.032**	268; 0.045
3.4×10^{16}	−2.71; −2.71	−2.69; −8.57	−2.49; −46.9	−2.39; −67.3	−2.26; −92	−2.06; −129
	0.019; 0.014	0.11; 0.008	6.3; 0.012	17.8; 0.015	49.3; 0.020	176; **0.030**

this value the growth rate is ∼0.4 nm s^{-1}, above this value the growth rate is in average about 0.03 nm s^{-1}. Following [17, 18] the electron temperature, $T_e = 2$e V, and the plasma density, $n_i = 10^{17}$ m^{-3}, are known by Langmuir probe measurements, T_i was allowed a range between 0.03 and 0.3 eV with the best agreement found at $T_i = 0.1$ eV. To justify this value above the neutral gas temperature, we note that dust clouds very often settle at the edge of sheaths (as in our case), striation, double layers, etc where ions have acquired a directional velocity in the corresponding presheath ($\lambda_{\text{mean free path}} = 150\,\mu$m). This directed velocity is rapidly made isotropic by few Coulomb collisions with the charged particles of the cloud. Moreover, our model is robust and will be hardly modified by a small amount of directed ion flow (see also figure 12 of [19]). While the density of the large particles is 2×10^{14} m^{-3}, the density of the small particles is not given.

First of all we verify our hypothesis. F can be derived from the carbon atoms sputtered from the electrode under ion bombardment; it is given by the discharge density of current multiplied by the yield (∼1%, see [18]) divided by the number of atoms in a small particle ($r_s = 1.5$ nm, we used a graphite-like density of 2000 kg m^{-3}). We obtain $F = 4.5 \times 10^{14}$ m^{-2} s^{-1}. Using $\theta_D = 5$ mm as the likely thickness of the dust cloud at the very edge of the negative glow we derive from equations (7) and (8) $\Gamma = 0.37$ nm s^{-1}, to compare with the experimental value: 0.4 nm s^{-1}.

Now, we are able to reproduce the full trend of Γ using our statistical model of charging. Table 1 gives the relevant values calculated for the given plasma parameters. Matching the growth rate of 0.4 nm s^{-1} at $r_{LD} = 45$ nm gives $n_{ds} = 8.5 \times 10^{16}$ m^{-3} (slightly above the electron density), and this value implies a fairly constant Γ, derived from equations (5), (7) and (8), for $r_s \gtrsim r_L < r_{LD}$. The theory also predicts a peak at $r_L = r_s$, due to the fact that initially the 's' and 'L' particles interact symmetrically, and the 'L' particle is as often positive as the 's' one, so that accretion events occur almost twice often as observed experimentally in [17]. At the experimental values of the cross over radius, the small particles' shortage reduces the growth rate in the saturation regime. Matching the observed Γ of 0.03 nm s^{-1} for $r_L > r_{LD}$ leads to densities n_{ds} around 0.35×10^{16} m^{-3}. The evolution of the system is shown in figure 4. The solid line represents the prediction of the theory, matching the experiments, just up to the cross

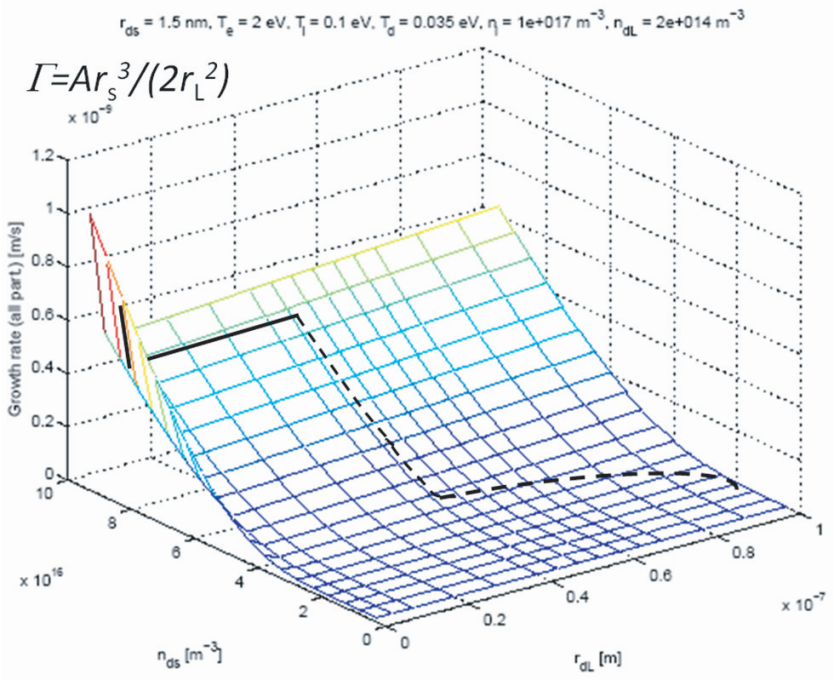

Figure 4. The dependence of the growth rate on the small particles density and the radius of the large particles in the hypothesis of bi-dispersed distribution of size. The solid curve corresponds to the results of this theory and describes the experimental parameters of table 1. The dashed curve carries on the evolution of the system after the cross over as derived from the experiments.

over. The theory includes a change of trend. The dashed line is merely the continuation of the evolution derived from the experiments.

We apply our model also to experiments done in different plasma, an RF discharge with graphite driven electrodes, described in [20]. As the Mie scattering strongly depends on the size, $\sim r^6$, we assume that the given density of particles corresponds to the larger size. The size evolution, as figure 4 of [20], shows a rapid growth in the first minute, $\sim$1–1.5 nm s^{-1} up to a size of $\sim$80 nm, followed in the next 2 min by saturation with a growth rate about 0.4 nm s^{-1}. We repeated the experiment, finding a good agreement with [20] to analyse the particulate by a high-resolution transmission electron microscope. Figure 5 shows a 'cauliflower' particle, with approximately 100 nm radius; looking at the details of the edges with higher magnification, it is possible to see the agglomeration of 3–5 nm particles. The 'cauliflower' structure, by itself, indicates an electrostatic attraction with attachment sensitive to the local electrostatic field. The only variable optimized was $T_i = 0.35$ eV, whereas $n_i = 5 \times 10^{16}$ m^{-3} is a typical value measured by Langmuir probe (far from the dust cloud). The production of smaller particles was derived from the C atoms sputtered from the electrode under ion bombardment, given by the Bohm flux, $J_{\mathrm{Bohm}} = n_i(k_B T_e/m_i)^{1/2} = 8 \times 10^{19}$ m^{-2} s^{-1}. With an average yield of 1%, 7×10^{13} m^{-2} s^{-1} small particles are continuously injected (again we used a graphite density of 2000 kg m^{-3}). Using $r_{\mathrm{ds}} = 1.5$ nm, $n_{\mathrm{dL}} = 5 \times 10^{14}$ m^{-3}, $T_e = 3$ eV and $T_d = 0.035$ eV, we find at the growth rate discontinuity (80 nm): $\bar{Q}_s = -0.64$e, $\bar{Q}_L = -35.1$e and $\Gamma = 0.96$ nm s^{-1}.

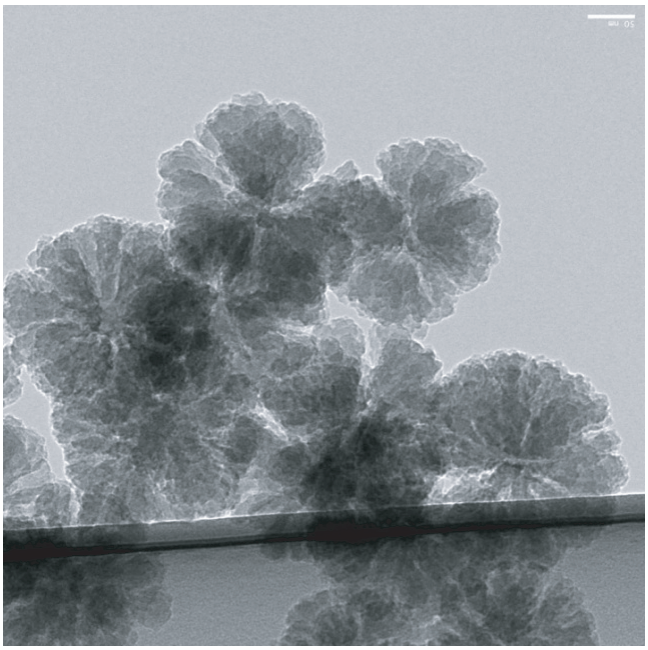

Figure 5. High-resolution transmission electron microscopy of a carbon particle collected after 7 min in RF discharge at $V_{\mathrm{rf(peak-peak)}} = 2\,\mathrm{kV}$ and 18 Pa. The reference sign corresponds to 50 nm.

At this point, the density of small particles approaches closely the plasma density and this is thought to cause an increase in the electron temperature [21]; we demonstrate that an increase in the electron temperature, in this energy range, enhances moderately the growth rate (with $T_{\mathrm{e}} = 8\,\mathrm{eV}$, $\Gamma = 1.24\,\mathrm{nm\,s^{-1}}$). The mono-dispersed distribution of size found in [20] provides another, indirect, validation of our theory. The agglomeration to large particles is much more likely than agglomeration of the small particles among themselves, see equation (5), and once some particles have started to grow in size both their density and accretion rate are practically constant.

Other applications include carbon dust formation in a continuous flow of argon–silane [21] or hydrogen–methane plasma (experiments in Garching) and many other ones. Lower the atomic weight of the gas, lower are the particle charges and more probable is the electrostatic agglomeration. We note here that we find agreement even with the experiments reported in [22] taking into account that the two size particles collected and analysed *ex situ* were generated in different places.

5. Conclusion

We explain the agglomeration of mesoscopic particles using a general theory based on charge fluctuations for ionized media with dispersed distribution of size. We benchmarked the theory with respect to experiments; a simplified model, based on a binary distribution of sizes, was able to reproduce the experimental observations, without the need to imply secondary electrons release. We realize that the given conditions for agglomeration, high density of particles and relatively high ion energy can only occur in complex plasmas of limited extension, at least in one

dimension. Given the reduced electron density ionization is mainly outside this complex plasma. Moreover, small particles and large particles are likely to coexist only at complex plasma edges.

Given the physical nature of the attraction this theory is applicable to most metal and dielectric materials in a huge variety of laboratory and natural environments.

References

[1] Bingham R and Tsytovich V N 2001 *Astron. Astrophys.* **376** L43
[2] Helling C, Klein R, Woitke P, Nowak U and Sedlmayr E 2004 *Astron. Astrophys.* **423** 657
[3] Selwin G S, Singh J and Bennet R S 1989 *J. Vac. Sci. Technol.* A **7** 2758
[4] Kasouit S, Damon-Lacoste J, Vanderhaghen R and Cabarrocas P R I 2004 *J. Non-Cryst. Solids* **338** 86
[5] Girard J P, Gulden W, Kolbasov B, Louzeiro-Malaquias A J, Petti D and Rodriguez-Rodrigo L 2008 *Nucl. Fusion* **48** 015008
[6] de Angelis U, Capobianco G, Marmolino C and Castaldo C 2006 *Plasma Phys. Control. Fusion* B **48** 91
[7] Khrapak S A, Nefedov A P, Petrov O F and Vaulina O S 1999 *Phys. Rev.* E **59** 6017
Khrapak S A, Nefedov A P, Petrov O F and Vaulina O S 1999 *Phys. Rev.* E **60** 3450 (erratum)
[8] Goree J 1994 *Plasma Sources Sci. Technol.* **3** 400
[9] Kortshagen U and Bhandarkar U 1999 *Phys. Rev.* E **60** 887
[10] Capasso F, Munday J N and Iannuzzi D 2007 *IEEE J. Sel. Top. Quantum Electron.* **13** 400
[11] Mendonça J T, Bingham R, Shukla P K and Resendes D 2001 *Phys. Lett.* A **289** 233
[12] Mendonça J T 2001 *Phys. Scr.* T **89** 55
[13] Allen J E 1992 *Phys. Scr.* **45** 497
[14] Allen J E, Annaratone B M and de Angelis U 2000 *J. Plasma Phys.* **63** 299
[15] Annaratone B M, Allen M W and Allen J E 1992 *J. Phys. D: Appl. Phys.* **25** 417
[16] van Kampen N G 1992 *Stochastic Processes in Physics and Chemistry* (Amsterdam: Elsevier) chapter 6
[17] Arnas C, Mouberi A, Hassouni K, Michau A, Lombardi G, Bonnin X, Bénédic F and Pégourié B 2009 *J. Nucl. Mater.* **390–391** 140
[18] Dominique C and Arnas C 2007 *J. Appl. Phys.* **101** 123304
[19] Fortov V E, Ivley A V, Khrapak S A, Khrapak A G and Morfill G E 2005 *Phys. Rep.* **421** 1
[20] Samsonov D and Goree J 1999 *Phys. Rev.* E **59** 1047
[21] Boufendi L and Bouchoule A 1993 *Plasma Sources Sci. Technol.* **2** 204
[22] Watanabe Y, Shiratani M, Kawasaki H, Singh S, Fukuzawa T, Ueda Y and Ohkura H 1996 *J. Vac. Sci. Technol.* A **14** 540